This article is published as part of the *Dalton Transactions* themed issue entitled:

Bridging the gap in catalysis *via* multidisciplinary approaches

Guest Editors: Christophe Coperet and Rutger van Santen
Université de Lyon, France and Eindhoven University of Technology, The Netherlands

Published in issue 36, 2010 of *Dalton Transactions*

Image reproduced with the permission of Dieter Vogt

Articles in the issue include:

Visit the *Dalton Transactions* website for more cutting-edge inorganic and organometallic research
www.rsc.org/dalton

Role of hydrogen in olefin isomerization and hydrogenation: a molecular beam study on Pd model supported catalysts

Wiebke Ludwig, Aditya Savara and Swetlana Schauermann*

The role of surface, and subsurface hydrogen species in olefin *cis-trans* isomerization and hydrogenation over a model Pd/Fe$_3$O$_4$/Pt(111) catalyst was investigated by pulsed molecular beam experiments and infrared reflection-absorption spectroscopy. We show that non-equivalent hydrogen species are involved in the two reaction pathways: whereas *cis-trans* isomerization proceeds with the surface hydrogen species, the presence of hydrogen absorbed in the subsurface region of Pd particles is required for the hydrogenation pathway. The activity and selectivity toward both reaction channels was found to significantly change on Pd particles when they are modified with strongly dehydrogenated carbonaceous deposits. Sustained hydrogenation activity was observed only on C-precovered particles, whereas sustained *cis-trans* isomerization proceeds on both C-free and C-containing catalyst. We discuss the possible microscopic origins of this effect.

1. Introduction

The conversion of olefins with hydrogen over transition metal surfaces, such as hydrogenation and *cis-trans* isomerization, is one of the most important reactions employed in industrial processes and catalysis research.[1,2] This type of reaction was extensively investigated in early years using conventional catalytic techniques,[3–5] and more recently by modern surface-science methodologies.[6–8] Although the surface-science approach has provided much insight into the mechanistic details of the key reaction steps on the catalyst surface, a complete microscopic understanding of the phenomena controlling the activity and selectivity in olefin conversions is still missing.

According to the generally accepted Horiuti-Polanyi reaction mechanism,[9] olefin conversions over transition metal catalysts proceed *via* a series of consecutive hydrogenation and dehydrogenation steps:
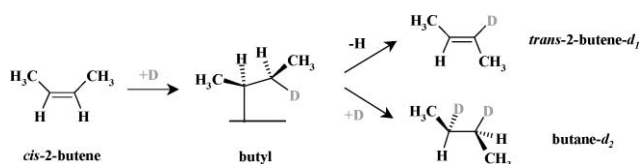
In the case of *cis*-2-butene, a 2-butyl-d_1 intermediate is formed in the first half-hydrogenation step, which is a common reaction intermediate for the *cis-trans* isomerization, the H/D exchange and the hydrogenation reaction pathways.[2,5,10] The 2-butyl-d_1 intermediate can undergo β-hydride elimination resulting in alkene formation, producing either the original molecule or a *cis-trans* isomerized molecule. When D$_2$ is used as a reactant, each *cis-trans* isomerization event is accompanied by substitution of one hydrogen atom with a deuterium (H/D exchange),[8]

allowing for a distinction between the reactant *cis*-2-butene and the product *trans*-2-butene-d_1 in the gas phase by using mass spectrometry. Alternatively, a second hydrogen (deuterium) atom can be inserted into the carbon metal bond of the 2-butyl-d_1 intermediate leading to the formation of butane-d_2. The adsorbed alkene as well as the 2-butyl-d_1 species may also dehydrogenate yielding other carbonaceous surface species, such as alkylidynes and other partly dehydrogenated carbonaceous deposits.[11,12]

There is an ongoing discussion on the role of the different hydrogen species in olefin conversions with hydrogen, which still remains a controversial issue. The traditional opinion that only surface hydrogen species are involved in the hydrogenation of the olefin double bond[2] was questioned for the first time by Ceyer *et al.*[13] More recent studies on supported nanoparticles provided the first experimental evidence that the weakly bound *subsurface/volume-absorbed* hydrogen species can be crucial for hydrogenation.[14,15] Specifically, a high hydrogenation activity was observed under low-pressure conditions on supported Pd clusters but not on the single crystals, which was attributed to the unique ability of the small particles to store large amounts of hydrogen atoms in a confined subsurface volume near the metal-gas interface. These recent findings clearly demonstrate the need for more precise catalytic systems to model the olefin conversions with hydrogen. In particular, studies on small metal nanoparticles supported on planar oxide substrates[16–19] under well-controlled conditions were envisioned to provide fundamental insights into the mechanisms of olefin hydrogenation and isomerization at the atomic scale. Such model systems allow us to introduce key complex features of real catalysts, without having to deal with the full complexity of the real system. In this contribution, we will report on the recent studies in our group, where well-defined supported model catalysts were utilized to unravel the microscopic details of olefin hydrogenation and *cis-trans* isomerization by using molecular beam (MB) methods in combination with infrared reflection-absorption spectroscopy (IRAS).

Fritz-Haber-Institut der Max-Planck-Gesellschaft, Faradayweg 4-6, 14195, Berlin, Germany

2. Experimental

All molecular beam (MB) and reflection-absorption infrared spectroscopy (IRAS) experiments were performed at the Fritz-Haber-Institut (Berlin) in an ultrahigh vacuum (UHV) apparatus described in detail previously.[20] A schematic representation of the setup is shown in Fig. 1a. Briefly, this system offers the experimental possibility of crossing up to three molecular beams on the sample surface. An effusive, doubly-differentially-pumped multi-channel array source was used to supply the D_2. This beam was modulated using remote-controlled shutters and valves. Beam fluxes for D_2 of 0.35 to 6.4×10^{15} molecules cm^{-2} s^{-1} (D_2 pressures from 0.4 to 5.3×10^{-6} mbar at the sample position) were used in these experiments. The source was operated at room temperature. The beam diameter was chosen such that it exceeded the sample diameter. A supersonic beam, generated by a triply-differentially-pumped source and modulated by a solenoid valve and remote-controlled shutter, was used to dose the *cis*-2-butene (Aldrich, >99%) at a flux of 5.6×10^{12} molecules cm^{-2} s^{-1} (typical backing pressure: 1.15 bar, pressure on the sample position 2.7×10^{-8} mbar). The diameter of the supersonic *cis*-2-butene beam was chosen to be smaller than the sample for the experiments discussed here. Modulation of the beams, in particular that of the *cis*-2-butene, was performed to differentiate between the products desorbing from the sample because of chemical reactions and any other interfering signals such as a slowly growing background observed over the course of the experiments. It should also be noted that the steady-state experiments reported below were carried out at temperatures well above those required for desorption of the olefins. Therefore, they reflect the kinetics of the chemical reactions on the surface, not that of the desorption of the hydrocarbons. An automated quadrupole mass spectrometer (QMS) system (ABB Extrel) was employed for the continuous and sequential monitoring of the partial pressures of the reactants (2-butene, $C_3H_5^+$ fragment at 41 a.m.u.) and products (2-butene-d_1, $C_3H_4D^+$ fragment at 42 a.m.u. and butane-d_2 $C_3H_5D_2^+$ fragment at 45 a.m.u.). All QMS data have been corrected to account for the natural abundance of ^{13}C in all the molecules followed in our experiments. IRAS data were acquired by using a vacuum Fourier-Transform Infrared (FT-IR) spectrometer (Bruker IFS 66v/S) with a spectral resolution of 2 cm^{-1}, using a mid-infrared (MIR) polarizer to select the p-component of the IR light.
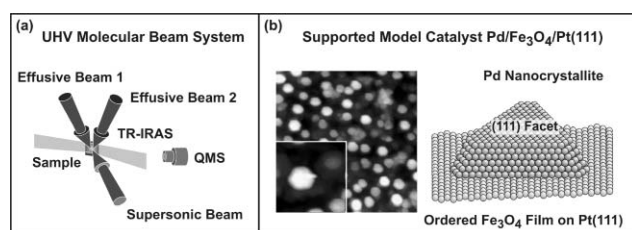

Fig. 1 (a) Schematic representation of the experimental setup for the molecular beam experiments. (b) Scanning tunneling microscopy (STM) image (100 nm × 100 nm, inset: 20 nm × 20 nm) of the Pd/Fe$_3$O$_4$/Pt(111) supported model catalyst used in the experiments described here,[24] together with a schematic representation of the structure of the supported Pd nanoparticles.

The Pd/Fe$_3$O$_4$ model catalyst was prepared as follows: the thin (~100 Å) Fe$_3$O$_4$ film was grown on a Pt(111) single crystal surface by repeated cycles of Fe (>99.99%, Goodfellow) physical vapor deposition and subsequent oxidation (see ref. 21–23 for details). The quality of the oxide film was checked by LEED and IRAS of CO. Pd particles (>99.9%, Goodfellow) were grown by physical vapor deposition using a commercial evaporator (Focus, EFM 3, flux calibrated by a quartz microbalance) while keeping the sample temperature fixed at 115 K. During Pd evaporation the sample was biased to + 800 V in order to avoid the creation of defects by metal ions. The final Pd coverage used in these experiments was 2.7×10^{15} atoms cm^{-2}. The resulting surfaces were then annealed to 600 K, and stabilized *via* a few cycles of oxygen (8×10^{-7} mbar for 1000 s) and CO (8×10^{-7} mbar for 3000 s) exposures at 500 K before use.[23] An STM image of the model surface resulting from this preparation is shown in Fig. 1b (from 24). The image displays Pd particles with an average diameter of 7 nm, containing approximately 3000 atoms each, and which cover the support uniformly with an island density of about 8.3×10^{11} islands cm^{-2}.[23] It should be noted that the size of the Pd particles appears substantially larger in these STM images because of the convolution of the signal with that of the tip used as the probe. An accurate estimate of Pd dispersion shows that only about 20% of the support surface area is covered with nanoparticles.[23] The majority of the particles are well-shaped crystallites grown in the (111) orientation and are predominantly terminated by (111) facets (~80%), but a small fraction of (100) facets (~20%) is also exposed. For carbon deposition, 0.85 Langmuir (1 L = 10^{-6} Torr·s) of *cis*-2-butene were adsorbed on Pd clusters pre-exposed to 280 L of D_2 at 100 K and decomposed by heating to 485 K (see ref. 25,26 for details).

3. Results and discussion

3.1. *cis*-2-butene conversion with deuterium on Pd/Fe$_3$O$_4$: isothermal molecular beam experiments

First, we investigate the conversion of *cis*-2-butene with deuterium over the Pd/Fe$_3$O$_4$ model catalyst as a function of temperature. For that, pulsed MB experiments were performed under isothermal conditions in the temperature range between 190 and 260 K. In this experiment, the sample was continuously exposed to a D_2 beam (pressure 4.0×10^{-6} mbar) during the complete experiment. Subsequently, the *cis*-2-butene (pressure 2.7×10^{-8} mbar) was switched on and off, starting 90 s after the beginning of the D_2 dosing. A typical MB sequence included 50 short butene pulses (4 s on, 4 s off time) followed by 30 longer pulses (20 s on, 10 s off time) (see ref. 25 for more details). The time evolution of the reactant trace (grey curve) and the production rate of *trans*-2-butene-d_1 (black curves) at different temperatures are displayed in Fig. 2; the start of the butene exposure corresponds to zero on the time axis. It is worth noting that no gas-phase reaction products were detected in identical isothermal MB experiments on the bare support, indicating that the Fe$_3$O$_4$ surface alone is inactive toward both hydrogenation and *cis-trans* isomerization of the alkene, in agreement with the previously reported lack of C–H bond activation in alkenes on Fe$_3$O$_4$.[27–29]

It should be pointed out that the formation of both reaction products *trans*-2-butene-d_1 and butane-d_2 begins after an induction period, as indicated in Fig. 2 by a dashed line. Previously, the origin of the induction period was investigated both on the
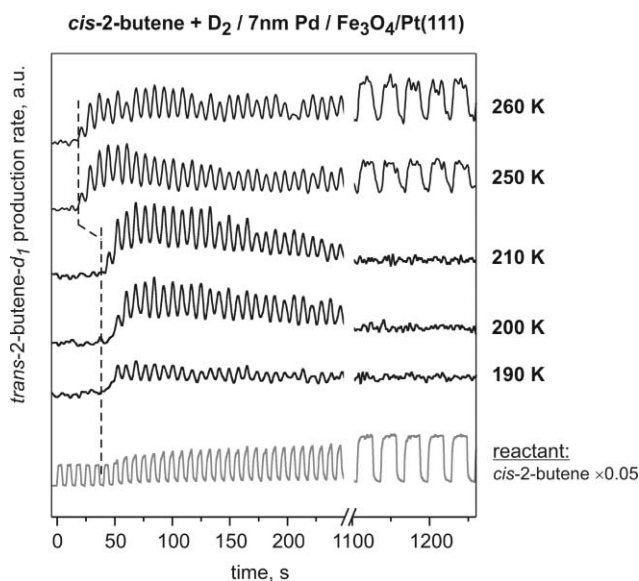
Fig. 2 Results from MB experiments carried out on Pd/Fe$_3$O$_4$ at different temperatures in the range from 190 to 260 K, using the MB pulse scheme described in the text. Shown is the time evolution of the product of *cis-trans* isomerization for each temperature (*trans*-2-butene-*d$_1$*, black curves) together with the reactant trace (*cis*-2-butene, gray curve). The dashed line indicates the end of the induction period. Below 210 K, the reaction rates are high initially but return to zero after prolonged olefin exposures. Above 250 K, there is a shorter induction period and sustained catalytic activity toward *cis-trans* isomerization is possible.

bare Fe$_3$O$_4$ support as well as on the Pd/Fe$_3$O$_4$ catalyst.[25] We attribute this effect to the initial irreversible adsorption of the reactant on the Fe$_3$O$_4$ support and to the molecular and/or dissociative adsorption of *cis*-2-butene on the Pd nanoparticles. Depending on the reaction temperature, partly dehydrogenated and/or molecular hydrocarbon species were suggested to be formed on the Pd particles that do not directly participate in but prepare the surface for the subsequent reactions. Only after the metal surface is saturated with those spectator hydrocarbon species does the butene catalytic conversion become possible. The duration of the induction period was found to depend on the reaction temperature, indicating that formation of the spectator hydrocarbon species involves a thermally activated step such as partial dehydrogenation. For more details, we refer the reader to the literature.[25]

Additionally, two temperature-dependent regimes of *cis-trans* isomerization can be identified. In the temperature range between 190 and 210 K, the transient behavior comprises an induction period and an initial high activity, followed by an asymptotic decay in reaction rate to zero after a few hundreds seconds. However, the reactivity pattern markedly changes when the reaction is carried out at 250 and 260 K. In this temperature region, a persistent catalytic activity towards *cis-trans* isomerization is observed even after prolonged periods of olefin exposure. In fact, the activity at these temperatures was probed for much longer time scales than that displayed in Fig. 2 without any significant reduction in the steady-state reaction rate of *cis-trans* isomerization.

The lack of sustained conversion in vacuum experiments is usually ascribed to the strong inhibition of dissociative H$_2$(D$_2$) adsorption on the metal surfaces induced by the presence of

strongly bonded hydrocarbon species.[2,30] Consistent with this is the fact that both hydrogenation and isomerization rates for *cis*-2-butene on Pt(111) follow a near-first-order dependence on the hydrogen pressure and a zero-order dependence on the hydrocarbon pressure.[31] In view of these results, we conclude that in the temperature region between 190 and 210 K the reaction observed in the initial stages of the MB runs involves only atomic D formed prior to *cis*-2-butene exposure. Once the hydrocarbon exposure starts, the butene appears to first form strongly adsorbed hydrocarbon surface species without any D consumption, until a threshold coverage of those species is reached. After this induction period, additional butene may react with D already present on the surface, leading to the initial high *cis-trans* isomerization rates. However, further dissociative adsorption of D$_2$ is inhibited by both the hydrocarbon deposits formed during early butene decomposition and molecularly adsorbed butene species, so the activity of the surface vanishes after the initially available D is consumed.

Following the same reasoning, it could be inferred that the sustained catalytic activity towards *cis-trans* isomerization observed above 250 K attests to the ability of the Pd particles to dissociatively adsorb D$_2$ at these temperatures, despite competition with butene adsorption and in the presence of partly dissociated hydrocarbon species on the surface. Two possible reasons might account for this phenomenon. First, faster butene desorption (as compared to the low temperature case) may result in a lower steady-state coverage of the reversibly-adsorbed butene, diminishing its potential poisoning effect on the dissociative adsorption of D$_2$. Second, more open metal sites might be present on the surface at higher temperatures because the more strongly dehydrogenated hydrocarbon spectator species formed above 250 K might have a smaller footprint. Both tendencies result in the reduced poisoning of the surface by hydrocarbons, and lead to the sustained ability of Pd particles to dissociatively adsorbed D$_2$ under reaction conditions.

In the low-temperature region, the time evolution profile of the hydrogenation product butane-*d$_2$* was found to be similar to that of the *cis-trans* isomerization pathway product: showing an induction period, initial high reactivity and vanishing reaction rates after prolonged olefin exposures (data not shown here). However, increasing the temperature above 250 K does not result in sustained hydrogenation activity in contrast with the persistent *cis-trans* isomerization at above 250 K. The microscopic origins of this phenomenon will be discussed in the following sections.

3.2 *cis*-2-butene conversion with deuterium on Pd/Fe$_3$O$_4$: reactivity of the C-containing surfaces

Accumulation of carbonaceous deposits resulting from the early decomposition of hydrocarbon reactants was recognized to considerably affect the activity and the selectivity in hydrocarbon conversions promoted by transition metals.[2,5,6,32] The underlying microscopic mechanisms of the carbon-induced changes in the reactivity remain as of yet unclear. To explore the role of carbon in olefin conversions, we prepared a model surface containing strongly dehydrogenated carbonaceous deposits (carbon) and performed reactivity measurements by pulsed MB experiments. To form the carbonaceous deposits, the sample was exposed to

280 L D_2 and 0.8 L *cis*-2-butene at 100 K and heated in vacuum to 500 K (see ref. 25 for details).

It has been recognized in the past that carbon species (produced by *e.g.* methanol decomposition[33,34]) are not uniformly distributed over the entire surface of the Pd nanoclusters but preferentially occupy the low-coordinated surface sites like edges, corners and to some extent (100) facets. To investigate the distribution of carbonaceous deposits produced in the C-deposition procedure followed in this work, we performed IRAS experiments using CO as a probe molecule for different adsorption sites. The IRAS spectra obtained on the clean and C-precovered Pd particles are shown in Fig. 3. The CO spectrum for the clean surface (bottom trace) is dominated by an intense and sharp peak centered around 1978 cm^{-1}, associated with Pd sites on the particle edges and corners and to a lesser extent with (100) facets.[35,36] The broad features between 1960 and 1800 cm^{-1} are attributed to CO adsorption on the regular (111) facets representing the majority of the surface sites.[35,36] It should be pointed out that the intensities of the IR signals are expected to be strongly modified by dipole-coupling effects[37] and, as a consequence, do not directly reflect the relative abundance of the corresponding sites. In the particular case of the Pd particles, the feature at high frequency corresponding to the low-coordinated sites (edges, corners, *etc.*) is likely to gain intensity at the expense of the absorption signal at lower frequency related to the regular (111) facets. In any case, the main effect of the deposition of carbonaceous species during the TPD runs reported here is the complete disappearance of the 1978 cm^{-1} peak; the spectral features in the low-frequency region remain nearly unchanged. Additionally, a new peak grows at 2095 cm^{-1}
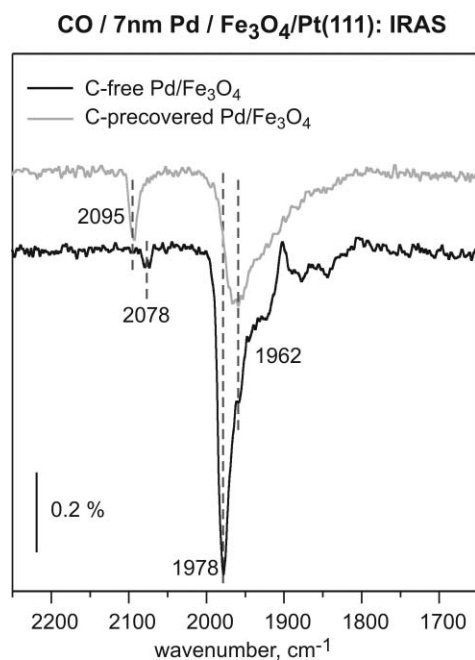
Fig. 3 CO IRAS titration spectra for Pd/Fe$_3$O$_4$/Pt(111) surfaces clean (bottom) and after carbon deposition (top). The surface was saturated with CO at room temperature and cooled down to 100 K before data acquisition. The data indicate that carbon is non-uniformly distributed over the Pd particles and blocks preferentially low-coordinated sites such as edges, corners and bridge sites on (100) facets. The majority of the surface sites on the regular (111) terraces remain unaffected.

associated with on-top adsorption sites. These changes indicate preferential adsorption of carbonaceous deposits on the edges, corners, and (100) facets, while regular terraces remain nearly carbon-free. Recent DFT calculations also support preferential adsorption of carbon at the edges of Pd clusters, and suggest that some of the carbon atoms may be located in subsurface sites.[38]

Next, the reactivity of the carbon-free and carbon-precovered surfaces was compared by applying the same pulse reaction scheme described in section 3.1. Fig. 4 displays the results of reaction rate measurements at 260 K for *cis-trans* isomerization and hydrogenation of *cis*-2-butene on the initially clean and carbon-precovered Pd particles. On the carbon-free surface a transient behavior is seen for both reaction pathways, as discussed in the previous section, consisting of an induction period in which no reaction products are detected and only the uptake of the reactant *cis*-2-butene is observed, followed by a period of high activity for both *cis-trans* isomerization and hydrogenation. However, whereas the *cis-trans* isomerization rate to *trans*-2-butene-d_1 is sustained over longer periods of time at this temperature, the hydrogenation rate to butane-d_2 returns to zero (Fig. 4a).
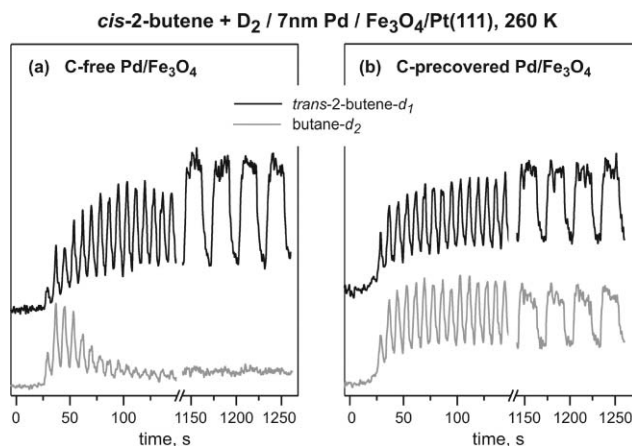
Fig. 4 Results from isothermal pulsed molecular beam experiments on the conversion of *cis*-2-butene with D_2 at 260 K on initially clean (a) and C-precovered (b) Pd/Fe$_3$O$_4$ model catalysts. Shown is the evolution of the reaction rates as a function of time for *trans*-2-butene-d_1 (black curves) and butane-d_2 (grey curves). The data indicate that while on the C-free surface only sustained isomerization is possible (left panel), both *cis-trans* isomerization and hydrogenation production persist on the surface precovered with carbon deposits (right panel).

In contrast, on the carbon-precovered surface not only *cis-trans* isomerization but also hydrogenation is maintained under steady-state conditions (Fig. 4b). This unique catalytic behavior clearly demonstrates the promoting role of carbon in the persistent hydrogenation activity of the Pd catalyst. It should be pointed out that the surface precovered with carbon also follows an induction period for the uptake of *cis*-2-butene, similar to that seen with the clean surface. This indicates that deposition of carbon does not significantly change the total surface area accessible for butene adsorption. This observation is corroborated by the CO-titration IR spectra obtained on both clean and carbon-precovered Pd particles (see Fig. 3): carbon contamination was found to affect mostly the low-coordinated (edges and corners of the Pd particles) without reducing the adsorption capacity of the (111) facets, which represent the majority of the surface sites.

In the steady state reaction regime (after prolonged *cis*-2-butene exposure), the two reaction pathways were found to exhibit very different transient behavior upon modulation of the olefin beam. Fig. 5 shows the time evolution of the reaction rates for isomerization (upper trace) and hydrogenation (lower trace) during the long pulses (20 s) of *cis*-2-butene on the carbon-precovered surface (averaged over the last 30 pulses). Note that prior to the beginning of each individual long pulse the surface was re-saturated with D so that the reactivity immediately after resuming the *cis*-2-butene beam corresponds to the reactivity of the catalyst saturated with D. The transient kinetic data show that the *cis-trans* isomerization rate simply follows the time evolution of the reactant. Since the β-hydride elimination step is generally believed to be fast as compared to the first-half hydrogenation of the olefinic double bond,[7] the *cis-trans* isomerization rate appears to be determined by the kinetics of butyl-d_1 formation, which in turn depends on the adsorption of the butene and the availability of dissociated D species. The constant *cis-trans* isomerization rate observed over the pulse length under these reaction conditions implies that the surface concentration of the butyl-d_1 reaction intermediate and the surface concentration of atomic D remain nearly constant over the duration of the reactant pulse. In contrast, the hydrogenation rate is high at the beginning of the *cis*-2-butene exposure but decreases considerably over the duration of the pulse. This behavior is typical for a reaction regime in which the availability of one of the reactants is high at the beginning time of the reaction but decreases as the reaction proceeds. In view of the fact that the surface concentration of the butyl-d_1 species remains constant (as indicated by the constant *cis-trans* isomerization rate), the decreasing hydrogenation rate seen towards the end of the pulse must be due to the depletion of the D species required for second-half hydrogenation of butyl-d_1. There is an apparent contradiction: on one hand, the decreasing hydrogenation rate indicates reduction of D availability toward the end of the *cis*-2-butene pulse; on the other hand, the constant *cis-trans* isomerization rate attests to the nearly constant concentration of D species. This contradiction can be solved only
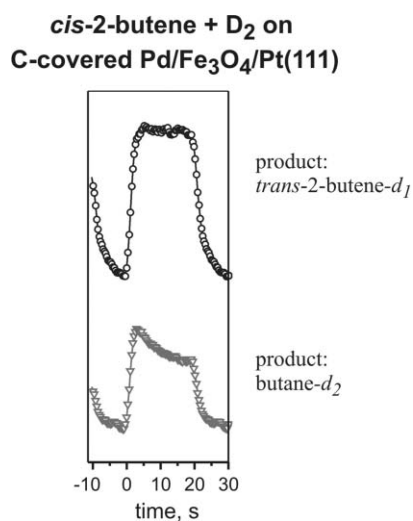
if we assume that non-equivalent D species participate in the first and the second half-hydrogenation of *cis*-2-butene. In this case, the concentration of the first type of D species required for butyl-d_1 formation remains nearly constant over the duration of the olefin pulse, whereas the second type of D species depletes in the course of reaction, resulting in decreasing hydrogenation rate. In the following section we will focus on unravelling the microscopic nature of these different D species.

It should be pointed out that our experimental data allow us to exclude some other possible explanations of the sustained hydrogenation on the C-modified particles. First, C-modification of the surface sites does not appear to noticeably enhance the intrinsic reactivity of the surface: neither for the *cis-trans* isomerization pathway, nor for the hydrogenation pathway. This follows from the observation of very similar initial reaction rates on the C-free and C-precovered surfaces when no limitations in D availability are present, *i.e.* on the D-saturated particles. Second, it appears unlikely that the sustained hydrogenation on C-precovered particles arises from modified binding properties of the hydrocarbon adsorbates (both butene and butyl-d_1 species) since reactivity of the *cis-trans* isomerization pathway – which proceeds through the same hydrocarbon intermediate – would be considerably influenced by C-deposition as well, which is not the case.

3.3 *cis*-2-butene conversion with deuterium on Pd/Fe₃O₄: role of surface and subsurface deuterium

From the experiments presented in the preceding section, two major closely related questions arise: (i) why is the hydrogenation pathway selectively suppressed under steady state reaction conditions on the carbon-free particles (see Fig. 4); and (ii) what is the role of carbon in the induction of the sustained hydrogenation activity on the C-modified catalyst? Additionally, the nature of the non-equivalent D species involved in the fist and the second half-hydrogenation steps, as indicated by the data presented in the Fig. 5, needs to be clarified.

As discussed above, the sustained *cis-trans* isomerization activity on the initially clean Pd particles implies that both the butyl-d_1 reaction intermediate and adsorbed D are available and that their surface concentrations remain nearly constant under steady state conditions at 260 K. Therefore the selectively vanishing hydrogenation activity strongly suggests that this pathway cannot solely be dependent on the apparently abundant *surface* D. It rather appears that the second half-hydrogenation of butyl-d_1 to butane-d_2 requires the presence of a specific type of D atoms, which are populated in the Pd particles saturated with D at the beginning of the reaction but cannot be replenished under the steady state conditions. In line with this reasoning, the decreasing hydrogenation activity over the butene pulse shown in the Fig. 5 suggests that two different non-equivalent D species have to be involved into the first and the second half-hydrogenation steps.

Generally, two different types of H(D) species are known to be formed on Pd: *surface* H(D) species are formed in a non-activated dissociative adsorption step and the *subsurface/volume-absorbed* H(D) species, which need to overcome an activation barrier to diffuse into the subsurface region.[39] Recently, the spatial distribution of H atoms in the supported Pd nanoclusters was addressed by hydrogen depth profiling *via* ¹H(¹⁵N, αγ)¹²C

cis-2-butene + D₂ on C-covered Pd/Fe₃O₄/Pt(111)

product: *trans*-2-butene-d_1

product: butane-d_2

Fig. 5 Average reaction rates measured for *cis-trans* isomerization (upper row) and hydrogenation (bottom row) at 260 K on C-precovered Pd catalysts. The rates were calculated by averaging the steady-state reaction rates of the last 30 long pulses of the experiment.

nuclear reaction analysis (NRA) to quantify the abundance of H species in the *surface-adsorbed* and *subsurface/volume-absorbed* states as a function of gas phase hydrogen pressure[40,41] (in the following, we will denote the *subsurface/volume-absorbed* state as *subsurface* state for simplicity). It has been determined that the population of the *subsurface* H species exhibits a strong pressure dependence up to at least 2×10^{-5} mbar, whereas the *surface* H coverage saturates as much lower pressures (below 1×10^{-6} mbar) and that the surface concentration does not change upon further pressure increase. Additionally, the quantities of Pd *subsurface-absorbed* H were found to be quite substantial when compared to the surface H saturation coverage, and even small H_2 pressure variations were observed to change the amount of *subsurface-absorbed* H on a scale equivalent to the total number of the *surface-adsorbed* H atoms. Previously, subsurface H species were suggested to participate in olefin hydrogenation.[14] However, a direct experimental proof of this hypothesis is still lacking.

In order clarify the possible involvement of the subsurface H(D) atoms in the second half-hydrogenation step, we carried out a series of transient MB experiments on the carbon-precovered Pd/Fe$_3$O$_4$/Pt(111) catalyst presented in the Fig. 6. The model catalyst was pre-exposed to D_2 and *cis*-2-butene to reach the steady state regime and then the D_2 beam was switched off for 100 s until the D reservoir on/in the Pd particles was depleted as indicated by vanishing reaction rates. Thereafter the D_2 beam was switched on again and the evolution of isomerization (*trans*-2-butene-d_1) and hydrogenation (butane-d_2) products was monitored as a function of time. This experiment was carried out for two different D_2 pressures (4×10^{-6} and 2×10^{-6} mbar) with a constant ratio $N_{D_2}:N_{cis\text{-}2\text{-butene}} = 570$, where N_{D_2} and $N_{cis\text{-}2\text{-butene}}$ are the numbers

of D_2 and *cis*-2-butene molecules impinging on the surface per time unit, respectively. In both cases all reaction rates returned to exactly the same levels as in the steady state regime before termination of the D_2 beam. However, the transient time evolution of the reaction products in the two pathways exhibits a very different behavior and D_2 pressure dependence. At both D_2 pressures the isomerization rate returns to the steady state level with a short and very similar characteristic time constant, *i.e.* $\tau_{char} = 11.0 \pm 0.3$ and 11.4 ± 0.3 s. In contrast, the evolution of the hydrogenation rate is substantially slower and exhibits a pronounced pressure dependence with characteristic times of 18.3 ± 0.3 s *versus* 28.3 ± 0.5 s at 4×10^{-6} and 2×10^{-6} mbar D_2, respectively. It should be emphasized that the time evolutions of the reaction products reflects the formation rates of atomic D species, *on* and *in* the Pd clusters, which accumulate only slowly on the surface covered with an excess of hydrocarbons because of hindered D_2 dissociation.

The fast and pressure-independent time evolution of the isomerization product suggests that this pathway is linked to the coverage of *surface* D atoms, which are expected to build up first upon resuming the D_2 beam due to the large heat of adsorption and to saturate at much lower pressures than the *subsurface-absorbed* D. The pronounced pressure dependence of the hydrogenation rate, on the other hand, identifies the D species involved in the second half-hydrogenation step as strongly sensitive to the D_2 pressure. In combination with the NRA results,[40] this observation strongly suggests that *subsurface/volume-absorbed* H(D) species are required for the second step in hydrogenation. It is also important to emphasize that the D species required for hydrogenation cannot be the *surface-adsorbed* D, as in this case the time evolution of butane-d_2 should be similarly pressure-independent as that of the isomerization product *trans*-2-butene-d_1. The substantially slower recovery of the hydrogenation rate as compared to *cis-trans* isomerization is a natural consequence of the fact that D atoms have to diffuse from the surface into the cluster volume, which is an activated process, whereas D_2 dissociation on Pd occurs spontaneously.[39] It is important to emphasize that the crucial role of the *subsurface/volume-absorbed* H(D) species for the hydrogenation route does not necessarily mean that these species are directly involved in the second half-hydrogenation step. Alternatively, the presence of *subsurface* H(D) might merely modify the adsorption and/or the electronic properties of surface H(D) making it more prone to react with alkyl species to form alkane.

Having established the nature of the H(D) atoms involved in the hydrogenation, we can now explain the observations displayed in Fig. 4. On the initially clean particles pre-saturated with D_2 prior to olefin exposure, both surface and subsurface D states are populated, which results in the high initial rates of both reaction pathways. After the prolonged olefin exposure, hydrogenation becomes selectively suppressed because the *subsurface* D species are consumed and cannot be replenished under the steady state reaction conditions. This inability to populate the subsurface D arises from the fact that during olefin exposure the surface D atoms can either diffuse into the particle volume or desorb and be consumed in the reaction with hydrocarbons. Apparently, the D diffusion into the bulk becomes negligible in presence of co-adsorbed hydrocarbons and therefore the hydrogenation rate vanishes.
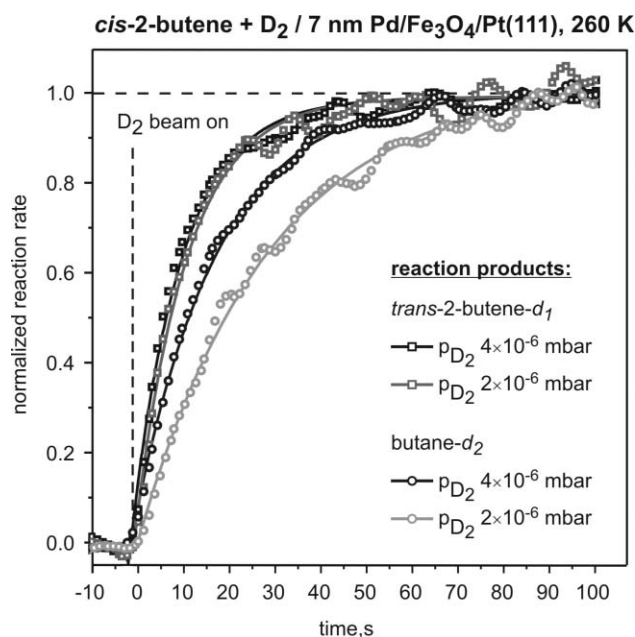

Fig. 6 Time evolution of the normalized reaction rates for the *cis-trans* isomerization (*trans*-2-butene-d_1) and hydrogenation (butane-d_2) products in the *cis*-2-butene + D_2 reaction after a temporary intermission of the D_2 beam. The reaction rates are obtained at 260 K over the C-precovered Pd/Fe$_3$O$_4$/Pt(111) catalyst at different D_2 pressures (2×10^{-6} and 4×10^{-6} mbar) with the ratio *cis*-2-butene:D_2 kept constant.

The sustained hydrogenation activity observed on the C-precovered catalyst suggests that this surface is capable of replenishing the subsurface D under steady state conditions even in presence of co-adsorbed hydrocarbons. This means that the co-adsorbed carbonaceous species (carbon) most likely facilitate the D diffusion from the surface into the particle volume. Recent theoretical calculation confirm the hypothesis that carbon adsorbed in the vicinity of particle's edges strongly reduces or nearly eliminates the activation barrier for subsurface hydrogen diffusion.[42] This effect was ascribed to a notable destabilization of surface H atoms on Pd nanoparticles in the presence of carbon and, more importantly, to C-induced expansion of the surface openings for penetration of H into subsurface region. In contrast, this effect was found to be considerably less pronounced on the intrinsically rigid regular Pd(111) surface.

An additional evidence for involvement of non-equivalent H(D) species into the first and second half-hydrogenation steps can be obtained from the D_2 pressure dependence of the *cis-trans* isomerization and hydrogenation rates. Fig. 7 displays the transient reactivity behavior over the duration of the *cis*-2-butene pulse for the isomerization (upper grey traces) and hydrogenation (lower black traces) pathways for five D_2 pressures 0.4, 0.9, 2.0, 4.0 and 5.3×10^{-6} mbar and the *cis*-2-butene pressure kept constant at 2.7×10^{-8} mbar with the corresponding ratios $N_{D_2}:N_{cis\text{-}2\text{-butene}}$ varying from 60 to 750. These data were obtained by averaging the response curves of the last 30 long pulses. Note that prior the beginning of each individual long pulse the surface was re-saturated with D_2 so that the reactivity immediately after resuming the *cis*-2-butene beam corresponds to the reactivity of the catalysts saturated with D. The reaction rates presented here were normalized to the same value for more convenient examination of the changes in the pulse shape with increasing D_2 pressure. At the highest presented D_2 pressure ($N_{D_2}:N_{cis\text{-}2\text{-butene}} = 750$, D_2 pressure 5.3×10^{-6} mbar), the

reaction rate of *cis-trans* isomerization displays a rectangular form following the time profile of the reactant butene, whereas the hydrogenation pathway shows high reaction rate at the beginning of the olefin exposure, which considerably decreases over the duration of the pulse. As discussed previously, the rectangular form of the response curve attests to the equal reaction rates on the D-saturated surface at the beginning of the pulse and on the surface under the steady state conditions reached during the pulse, and with this suggests that adsorption of hydrocarbon species does not negatively affect the surface concentration of D under steady state conditions. At the lowest $N_{D_2}:N_{cis\text{-}2\text{-butene}}$ ratios (60 and 130, D_2 pressures 0.4 and 0.9×10^{-6} mbar), the pulse shape of the *cis-trans* isomerization rate changes and shows a behavior typical for D-deficient conditions with the transient rate on the D-saturated surface somewhat higher than the steady state reaction rate. Apparently, under such conditions the concentration of *surface* D species decreases during the olefin pulse. The most likely reason for this can be inhibition of dissociative D_2 adsorption by high concentrations of co-adsorbed hydrocarbon species.[43] Note that under all conditions applied in these experiments the reaction is carried out in a large excess of D_2 in the gas phase with the reactant ratios $N_{D_2}:N_{cis\text{-}2\text{-butene}} = 60$–750, so that the decrease of the reaction rates cannot be explained simply by limited supply of molecular deuterium from the gas phase. In the entire $N_{D_2}:N_{cis\text{-}2\text{-butene}}$ range, the form of the *cis-trans* isomerization profile smoothly changes from the non-rectangular one at low ratios to the rectangular one at the highest $N_{D_2}:N_{cis\text{-}2\text{-butene}}$ ratios (Fig. 7). Such a trend attests to the change of the rate determining step with increasing $N_{D_2}:N_{cis\text{-}2\text{-butene}}$ ratio: whereas at low reactant ratios (*i.e.* at low D_2 pressures) the reaction runs under the D-deficient conditions and is limited by the formation of *surface* D species, at high reactant ratios there are no limitations in D availability and the isomerization rate is most likely determined by the formation of butyl-d_1 species (see discussion above).

In contrast, the hydrogenation profiles remain very similar for all investigated D_2 pressures. In this pathway, the reaction rate drops by ~ 30% from the initial value after 20 s olefin exposure for all reaction D_2 pressures. It is important to point out that there is no correlation between the pulse profile of both reaction pathways: whereas a smooth transition from the D-deficient to D-rich conditions is observed for *cis-trans* isomerization with increasing D_2 pressure, the hydrogenation profile remains the same in the whole pressure range. This observation strongly suggests that the hydrogenation path is governed by the time evolution of some special kind of D species, which are *not identical* to the *surface* ones. Obviously, the formation of this type of D species is slow under all investigated conditions, even at high D_2 pressures, where no limitations in availability of the *surface* D species is observed as indicated by rectangular pulse profiles of *cis-trans* isomerization. This observation is in line with our conclusions from the pulsed MB experiments described above recognizing the presence of *subsurface* D species as a necessary condition for hydrogenation to proceed. It should be emphasized, however, that the exact role of the subsurface H(D) species in the second half-hydrogenation of the alkyl intermediate is not clear yet: it can be speculated that subsurface H(D) participates in the reaction itself or that it merely changes the adsorption and/or electronic properties of the *surface* H(D) species making it more prone to attack the carbon-metal bond. Further theoretical work is needed
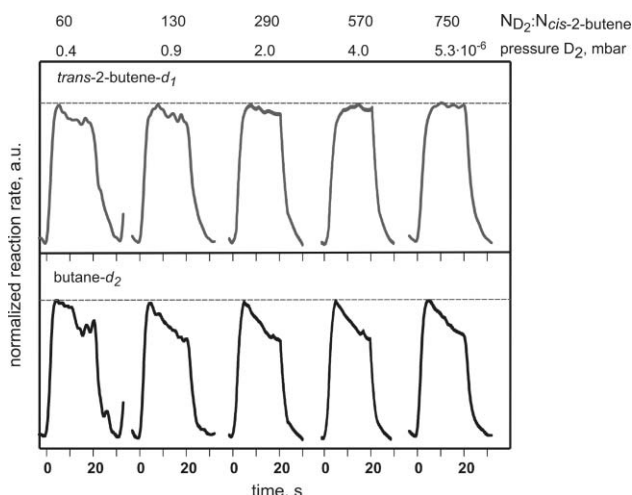

Fig. 7 Normalized averaged reaction rates obtained at different D_2 pressures (0.4, 0.9, 2.0, 4.0 and 5.3×10^{-6} mbar). Shown are the rates for the *cis-trans* isomerization (grey traces) and hydrogenation (black traces) pathways. At the two lowest D_2 pressures, the decaying pulse profiles point to D-deficient conditions for both reaction pathways, whereas at the highest D_2 pressure (5.3×10^{-6} mbar) only the hydrogenation rate decreases over the duration of the *cis*-2-butene pulse while the *cis-trans* isomerization pulse exhibit the rectangular form.

to understand the microscopic picture of this process in more detail.

The fact that the population of this species decreases during the olefin puls even at high D_2 pressures, where no limitations in availability of the *surface* D species is observed, indicates that co-adsorbed hydrocarbons negatively affect D diffusion into subsurface. It can be speculated that this result is a consequence of competition between activated subsurface diffusion on one hand and deuterium desorption and consumption in the reaction with hydrocarbon on the other hand.

Conclusions

The catalytic conversion of *cis*-2-butene with deuterium on a well-defined model supported catalyst consisting of Pd particles deposited on a well-ordered Fe_3O_4/Pt(111) was investigated under UHV conditions by using a combination of pulsed molecular beam experiments and infrared reflection-absorption spectroscopy. Emphasis was placed on the elucidation of the role of different H(D) species in two possible reaction pathways – *cis-trans* isomerization and hydrogenation. Additionally, the influence of the carbonaceous deposits typically present under catalytic reaction conditions on the activity and selectivity in these reactions was explored. We provide clear experimental proof that hydrogenation of the olefinic double bond requires the presence of weakly bound hydrogen species absorbed in the Pd particle volume. In contrast, the *cis-trans* isomerization pathway was found to proceed with the surface-adsorbed H(D) species. Deposition of carbon—which was spectroscopically shown by CO adsorption to preferentially adsorb at the low-coordinated surface particle sites such as edges and corners—crucially affects the activity of Pd clusters in hydrogenation. Only in presence of these strongly dehydrogenated carbonaceous deposits do Pd clusters exhibit an ability to maintain hydrogenation activity at the initially high level observed on a D-saturated catalyst. Activity for the *cis-trans* isomerization is also maintained on the C-covered catalyst. Conversely, on the C-free surface, only *cis-trans* isomerization can proceed over long periods of time, whereas the hydrogenation pathway becomes selectively suppressed after a short period of initial high activity. We attribute this difference to the ability of C-covered Pd clusters to more efficiently replenish the reservoir of subsurface hydrogen species required for hydrogenation under the steady state reaction conditions. Apparently, the subsurface H(D) diffusion is inhibited on the C-free clusters resulting in zero hydrogenation rates, whereas C deposition leads to faster H(D) subsurface diffusion and allows with this to maintain the hydrogenation rate in the steady state.

Acknowledgements

References

1 V. Ponec and G. C. Bond, *Catalysis by Metals and Alloys*, Elsevier, Amsterdam, 1995.
2 G. C. Bond, *Metal-Catalysed Reactions of Hydrocarbons*, Springer Science, New York, 2005.
3 T. I. Taylor, in *Catalysis*, ed. P. H. Emmett, Reinhold, New York, 1957, Vol. 5, pp. pp. 257–403.
4 C. Kemball, In *Advances in Catalysis and Related Subjects*, ed. D. D. Eley, P. W. Selwood and P. B. Weisz, Academic Press: New York, 1959, Vol. 11, pp. 223–262.
5 J. Horiuti, K. Miyahara, *Hydrogenation of Ethylene on Metallic Catalysts*, Report NSRDS-NBC No. 13, National Bureau of Standards, 1968.
6 G. A. Somorjai, *Introduction to Surface Science Chemistry and Catalysis*, John Wiley & Sons, New York, 1994.
7 F. Zaera, *Prog. Surf. Sci.*, 2001, **69**, 1.
8 Z. Ma and F. Zaera, *Surf. Sci. Rep.*, 2006, **61**, 229.
9 J. Horiuti and M. Polanyi, *Trans. Faraday Soc.*, 1934, **30**, 1164.
10 F. Zaera, *Chem. Rev.*, 1995, **95**, 2651.
11 R. J. Koestner, J. C. Frost, P. C. Stair, M. A. Van Hove and G. A. Somorjai, *Surf. Sci.*, 1982, **116**, 85.
12 F. Zaera, *Langmuir*, 1996, **12**, 88.
13 S. P. Daley, A. L. Utz, T. R. Trautman and S. T. Ceyer, *J. Am. Chem. Soc.*, 1994, **116**, 6001.
14 A. M. Doyle, Sh. K. Shaikhutdinov, S. D. Jackson and H.-J. Freund, *Angew. Chem., Int. Ed.*, 2003, **42**, 5240.
15 A. M. Doyle, S. K. Shaikhutdinov and H.-J. Freund, *Angew. Chem., Int. Ed.*, 2005, **44**, 629.
16 M. Bäumer and H.-J. Freund, *Prog. Surf. Sci.*, 1999, **61**, 127.
17 H.-J. Freund, *Surf. Sci.*, 2002, **500**, 271.
18 H.-J. Freund, *Angew. Chem., Int. Ed. Engl.*, 1997, **36**, 452.
19 H.-J. Freund and G. Pacchioni, *Chem. Soc. Rev.*, 2008, **37**, 2224.
20 J. Libuda, I. Meusel, J. Hartmann and H.-J. Freund, *Rev. Sci. Instrum.*, 2000, **71**, 4395.
21 W. Weiss and W. Ranke, *Prog. Surf. Sci.*, 2002, **70**, 1.
22 C. Lemire, R. Meyer, V. Henrich, S. K. Shaikhutdinov and H.-J. Freund, *Surf. Sci.*, 2004, **572**, 103.
23 T. Schalow, B. Brandt, M. Laurin, S. Schauermann, J. Libuda and H.-J. Freund, *J. Catal.*, 2006, **242**, 58.
24 T. Schalow, B. Brandt, D. E. Starr, M. Laurin, S. Schauermann, S. K. Shaikhutdinov, J. Libuda and H.-J. Freund, *Catal. Lett.*, 2006, **107**, 189.
25 B. Brandt, J.-H. Fischer, W. Ludwig, J. Libuda, F. Zaera, S. Schauermann and H.-J. Freund, *J. Phys. Chem. C*, 2008, **112**(30), 11408.
26 B. Brandt, W. Ludwig, J.-H. Fischer, J. Libuda, F. Zaera and S. Schauermann, *J. Catal.*, 2009, **265**, 191.
27 C. Kuhrs, Y. Arita, W. Weiss, W. Ranke and R. Schlögl, *Top. Catal.*, 2000, **14**, 111.
28 D. Zscherpel, W. Ranke, W. Weiss and R. Schlögl, *J. Chem. Phys.*, 1998, **108**, 9506.
29 Y. Joseph, M. Wühn, A. Niklewski, W. Ranke, W. Weiss, Ch. Wöll and R. Schlögl, *Phys. Chem. Chem. Phys.*, 2000, **2**, 5314.
30 F. Zaera and G. A. Somorjai, in *Hydrogen Effects in Catalysis: Fundamentals and Practical Applications*, ed. Z. Paál, P. G. Menon, Marcel Dekker, New York, 1988, pp. 425–447.
31 Ch. Yoon, M. X. Yang and G. A. Somorjai, *J. Catal.*, 1998, **176**, 35.
32 G. C. Bond and P. B. Wells, *Adv. Catal.*, 1965, **15**, 91.
33 S. Schauermann, J. Hoffmann, V. Johánek, J. Hartmann, J. Libuda and H.-J. Freund, *Angew. Chem., Int. Ed.*, 2002, **41**, 2532.
34 S. Schauermann, J. Hoffmann, V. Johánek, J. Hartmann, J. Libuda and H.-J. Freund, *Catal. Lett.*, 2002, **84**, 209.
35 K. Wolter, O. Seiferth, H. Kuhlenbeck, M. Bäumer and H.-J. Freund, *Surf. Sci.*, 1998, **399**, 190.
36 M. Frank and M. Bäumer, *Phys. Chem. Chem. Phys.*, 2000, **2**, 4265.
37 P. Hollins, *Surf. Sci. Rep.*, 1992, **16**, 51.
38 I. V. Yudanov, K. M. Neyman and N. Rösch, *Phys. Chem. Chem. Phys.*, 2004, **6**, 116.
39 K. Christmann, *Surf. Sci. Rep.*, 1988, **9**, 1.
40 M. Wilde, K. Fukutani, W. Ludwig, B. Brandt, J.-H. Fischer, S. Schauermann and H.-J. Freund, *Angew. Chem., Int. Ed.*, 2008, **47**, 9289.
41 M. Wilde, K. Fukutani, M. Naschitzki and H.-J. Freund, *Phys. Rev. B: Condens. Matter Mater. Phys.*, 2008, **77**, 113412.
42 K. M. Neyman and S. Schauermann, *Angew. Chem., Int. Ed.*, 2010, DOI: 10.1002/anie.200904688.
43 Note that the shown pulse profiles are the average of 30 independent nearly identical pulses, *i.e.* after the interruption of the olefin exposure the deuterium beam restores the surface to its original highly reactive state. Therefore the decreasing reaction rate over the olefin pulse cannot be associated with irreversible changes of the surface such as *e.g.* contamination.